

Month 2018 Rapid and Selective Detection of Cyanide Anion by Enhanced Fluorescent Emission and Colorimetric Color Changes at Micromole Levels in Aqueous Medium

Wen-Juan Qu, Wen-Ting Li, Hai-Li Zhang, Tai-Bao Wei, Qi Lin, Hong Yao, and You-Ming Zhang* 

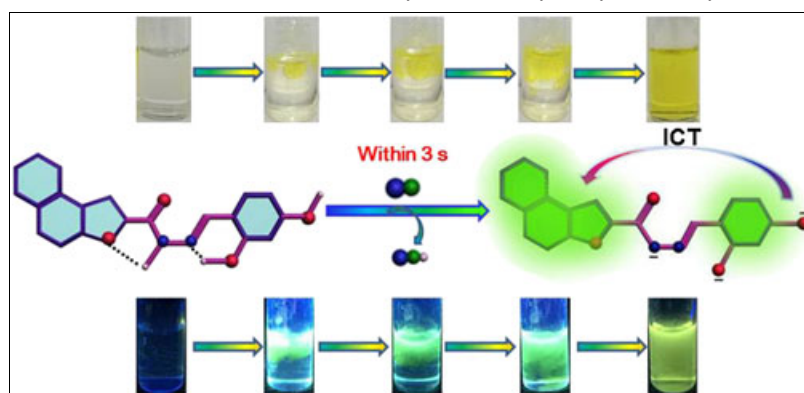
Key Laboratory of Eco-Environment-Related Polymer Materials, Ministry of Education of China, Key Laboratory of Polymer Materials of Gansu Province, College of Chemistry and Chemical Engineering, Northwest Normal University, Lanzhou, Gansu 730070, People's Republic of China

*E-mail: zhangnwnu@126.com

Received November 2, 2017

DOI 10.1002/jhet.3113

Published online 00 Month 2018 in Wiley Online Library (wileyonlinelibrary.com).



One main source of cyanide (CN^-) exposure for mammals is through the plant consumption; thus, the sensitive and selective cyanide detection in plant tissue is a significant and urgent work. Here, a simple sensor *N*'-(2,4-dihydroxybenzylidene)naphtha[2,1-*b*]furan-2-carbohydrazone (**Q1-3**) was designed and synthesized for selective and sensitive dual-channel detection of cyanide in aqueous medium (DMSO/ H_2O , 1:9, v/v). Acylhydrazone and phenolic hydroxyl groups on **Q1-3** are the recognition sites, and naphthofuran group is the signal report group. The intramolecular charge transfer between the benzene group and naphthofuran group was impeded because of the electron-withdrawing groups (hydroxyl) on sensor **Q1-3**. Interestingly, the sensor **Q1-3** exhibited an intramolecular charge transfer absorption band at 400 nm and emission band at 500 nm, respectively, directly realizing an “OFF–ON” response after the deprotonation process induced by cyanide anions in aqueous medium (DMSO/ H_2O , 1:9, v/v). Notably, this sensor was successfully applied to detect cyanide anions in food samples, which proves a very simple and selective platform for on-site monitoring of cyanide in agriculture samples. In addition, the test strips and silica gel plates based on **Q1-3** were also fabricated, which could act as test kits and silica gel plates for convenient and efficient detection of cyanide anions.

J. Heterocyclic Chem., **00**, 00 (2018).

INTRODUCTION

Recognition of trace amounts of cyanide in biological and environmental samples by simple and sensitive methods is an area of immense interest due to the extreme toxicity of cyanide at low concentrations [1–8]. The toxicity of cyanide to mammals is mainly derived from its propensity to bind with the iron in cytochrome oxidase, thus inducing the inhibition of mitochondrial electron chain transport and change of the cellular redox state [9,10]. One main source of cyanide exposure for mammals is through the consumption of certain foods and plants. Therefore, it is significant to monitor cyanide in plant tissues [11,12]. It is well known that 0.5–3.5 mg/kg of body weight is lethal for humans. According to the World Health Organization, water having cyanide concentrations lower than 1.9 μM are acceptable for

drinking [13]. Several analytical methods such as voltammetry, potentiometry, and chromatography have been used for cyanide detection [14–16]. These methods can successfully detect cyanide anions at very low levels ($< 0.1 \mu\text{M}$) but need tedious sample pretreatment or expensive instrumentation [17]. Whereas chemical sensors provide another approach, which is simple, inexpensive, and rapid in real-time monitoring of cyanide anions [18–23]. The sensing process is often accompanied by changes in absorption or fluorescence spectra that can be precisely monitored and sometimes detected by the naked eyes [24–34]. Although various fluorescence probes have been reported for cyanide anions, the detection of endogenous biological cyanide in plant tissue remains to be explored because of the high background signal and large thickness of plant tissue that hamper the effective application of traditional one-photo excitation. Among

various types of sensors reported so far, only few of them can detect cyanide anions in high water-content systems.

In order to solve these problems about cyanide anion detection, we designed and synthesized a simple chemosensor **Q1-3**, which can selectivity and sensitivity dual-channel detect cyanide anions in aqueous medium (DMSO/H₂O, 1:9, v/v). The intramolecular charge transfer (ICT) between the benzene group and naphthofuran group was impeded because of the electron-withdrawing groups (hydroxyl) on sensor **Q1-3**. The sensor **Q1-3** exhibited an ICT absorption band at 400 nm and emission band at 500 nm, respectively, directly realizing an “OFF–ON” response after the deprotonation process induced by cyanide anions in aqueous medium (DMSO/H₂O, 1:9, v/v). There is an obvious color change from colorless to yellow in visible light and a bright yellow green fluorescent, which can be seen by naked eyes under the UV lamp (365 nm) after the addition of cyanide anions to the solution of **Q1-3**. Notably, this sensor was successfully applied to detect cyanide in food samples, which proves a very simple and selective platform for on-site monitoring of cyanide in agriculture samples. In addition, the test strips and silica gel plates based on **Q1-3** were fabricated, which could act as convenient and efficient cyanide test kits and silica gel plates.

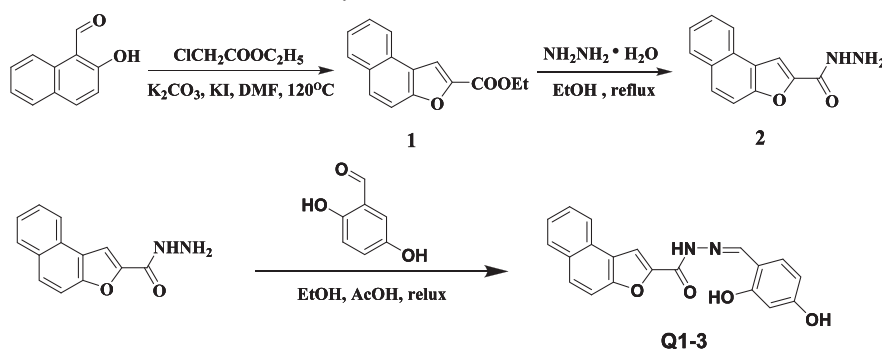
EXPERIMENTAL

Materials and physical methods. Fresh double-distilled water was used throughout the experiments. All other reagents and solvents were commercially available at analytical grade and were used without further purification. ¹H-NMR and ¹³C-NMR spectra were recorded on an Agilent DD2 at 600-MHz spectra. ¹H chemical shifts are reported in ppm downfield from tetramethylsilane (δ scale) with the solvent resonances as internal standards. Ultraviolet–visible (UV–vis) spectra

were recorded on a Shimadzu UV-2550 spectrometer. Photoluminescence spectra were performed on a Shimadzu RF-5301 fluorescence spectrophotometer. Melting points were measured on an X-4 digital melting point apparatus. The infrared spectra were performed on a Digilab FTS-3000 Fourier transform infrared spectrophotometer.

Synthesis of sensor molecule Q1-3. Compound **Q1-3** can be readily prepared by a simple and low-cost amide reaction between naphtha[2,1-*b*]furan-2-carbohydrazide and 2,5-dihydroxybenzaldehyde (Scheme 1). 2-Hydroxy-1-naphthaldehyde (0.86 g, 5 mmol) and K₂CO₃ (1.38 g, 10 mmol) were mixed in 20 mL dimethylformamide (DMF), ethyl chloroacetate (0.72 g, 6 mmol) and KI (0.09 g, 0.6 mmol) were mixed in 10 mL DMF and stirred at room temperature for 30 min, and then the latter slowly dripped into the former. The solution was stirred for 4 h at 90°C and stirred continuously after the temperature was increased to 120°C. After cooling to room temperature, the solution was poured into 200 mL distilled water, and the white precipitate was filtered, washed three times with hot absolute ethanol, and then obtained compound **1**. Next, compound **1** (1.14 g, 5 mmol) and hydrazine hydrate (0.50 g, 10 mmol) were mixed in 30 mL EtOH; the solution was stirred under reflux for 24 h at 85°C. After cooling to room temperature, the yellow precipitate was filtered, washed three times with hot absolute ethanol, and then obtained compound **2**. Naphtha[2,1-*b*]furan-2-carbohydrazide (**2**) (0.45 g, 2 mmol), 2,5-dihydroxybenzaldehyde (0.35 g, 2.5 mmol), and 2.5 mL glacial acetic acid (AcOH) were mixed in hot EtOH (30 mL). The solution was stirred under reflux for 6 h. After cooling to room temperature, the yellow precipitate was filtered, washed three times with hot absolute EtOH, and then recrystallized with EtOH/DMF to give a yellow powder product **Q1-3** (1.45 mmol) in 72.3% (mp >300°C). IR: (KBr, cm⁻¹) ν : 3244 (acylhydrazone –NH), 2989 (phenol –OH), 1640 (C=O), 1595 (C=C). ¹H-NMR (DMSO-*d*₆, 600 MHz)

Scheme 1. Synthesis of the sensor molecule **Q1-3**.



δ 12.35/ppm (s, 1H, phenol –OH on ortho-position –OH), δ 10.02/ppm (s, 1H, phenol –OH on para-position –OH), δ 11.36/ppm (s, 1H, imide –NH), δ 7.35–8.63/ppm (m, 9H, ArH), δ 6.35–6.40/ppm (m, 3H, PrH). ^{13}C -NMR (DMSO- d_6 , 150 MHz) δ /ppm 161.36, 159.94, 154.55, 152.86, 150.11, 147.76, 131.71, 130.56, 129.31, 128.97, 127.92, 127.80, 125.93, 124.16, 123.12, 112.95, 111.04, 110.87, 108.27, 103.11. Electrospray ionization mass spectrometry calcd for $\text{C}_{20}\text{H}_{14}\text{N}_2\text{O}_4 + \text{H}^+$ 347.16; found 346.10.

General procedure for ultraviolet–visible experiments.

All the UV–vis experiments were carried out in DMSO/ H_2O (1:9, v/v) solution on a Shimadzu UV-2550 spectrometer. Any changes in the UV–vis spectra of the synthesized compound were recorded on addition of tetrabutylammonium salts while keeping the ligand concentration constant ($2.0 \times 10^{-5} \text{ M}$) in all experiments. Tetrabutylammonium salt ($1.0 \times 10^{-3} \text{ M}$) of anions (F^- , Cl^- , Br^- , I^- , AcO^- , H_2PO_4^- , HSO_4^- , and ClO_4^-) and sodium salt ($1.0 \times 10^{-3} \text{ M}$) of anions (CN^- and SCN^-) were used for the UV–vis experiments.

General procedure for fluorescence spectra experiments.

All the fluorescence spectroscopy was carried out in DMSO/ H_2O (1:9, v/v) solution on a Shimadzu RF-5301 spectrometer. Any changes in the fluorescence spectra of the synthesized compound were recorded on addition of tetrabutylammonium salts while keeping the ligand concentration constant ($2.0 \times 10^{-5} \text{ M}$) in all experiments. Tetrabutylammonium salt ($1.0 \times 10^{-3} \text{ M}$) of anions (F^- , Cl^- , Br^- , I^- , AcO^- , H_2PO_4^- , HSO_4^- , and ClO_4^-) and sodium salt ($1.0 \times 10^{-3} \text{ M}$) of anions (CN^- and SCN^-) were used for the fluorescence experiments.

General procedure for ^1H -NMR experiments. For ^1H -NMR titrations, the solution of **Q1-3** was prepared in DMSO- d_6 and the appropriate concentrated solution of guest was prepared in deuterium water. Aliquots of the two solutions were mixed directly in NMR tubes.

RESULTS AND DISCUSSION

To evaluate the real-time detection ability of sensor **Q1-3** towards various anions (such as F^- , Cl^- , Br^- , I^- , AcO^- , H_2PO_4^- , HSO_4^- , ClO_4^- , SCN^- , and CN^-), changes in the absorption and fluorescence spectra were measured immediately upon adding various anions to the solutions of sensor **Q1-3**.

As illustrated in Figure 1, sensor **Q1-3** exhibited a maximum absorption band at 335 nm. The addition of cyanide led to significant decrease of this band accompanied with the emergence of three new absorption bands at 400, 418, and 442 nm, respectively, while other anions caused no influence in the absorption spectra. Owing to the appearance of the new band in the visible

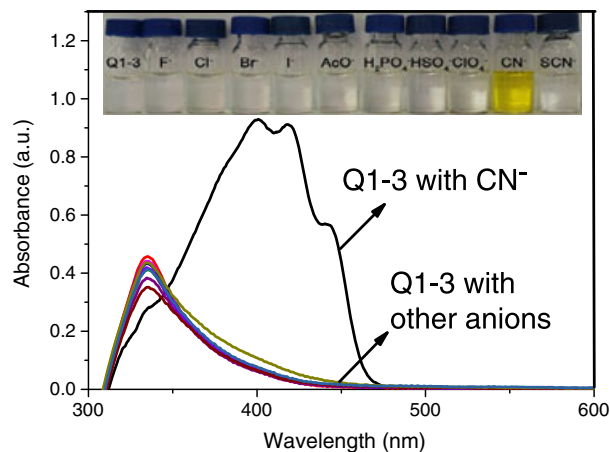


Figure 1. Absorbance spectra of compound **Q1-3** ($20 \mu\text{M}$) in DMSO/ H_2O (1:9, v/v) in the presence of cyanide and other anions (50 equiv). Inset: photograph showing the change in color of the solution of **Q1-3** in DMSO/ H_2O (1:9, v/v, $20 \mu\text{M}$) after addition of cyanide and other anions at room temperature. [Color figure can be viewed at wileyonlinelibrary.com].

region, the changes could be observed by naked eyes. The colorless solution of sensor **Q1-3** turned to yellow in the presence of cyanide. In contrast, other anions (especially F^- , AcO^- , H_2PO_4^- , and SCN^-) did not induce any spectral and color changes.

On the other hand, sensor **Q1-3** represented weak fluorescence emission in the solution, because of the efficient electron withdrawing of phenolic hydroxyl groups. However, a prominent fluorescence enhancement at 500 nm appeared after the addition of cyanide to the solution of **Q1-3**. Meanwhile, other anions caused no significant influence about the fluorescent spectra of sensor **Q1-3**, which could not be detected by naked eyes under the UV lamp. According to these results, it indicated that sensor **Q1-3** could recognize cyanide anions selectively through colorimetric and fluorimetric dual channels in real time. In addition, no significant changes were observed after the addition of other anions (Fig. 2).

In order to further investigate the practical applicability of **Q1-3** as a cyanide sensor, we carried out competitive experiments in the presence of 50 equiv of cyanide anions and 50 equiv of other anions in the solution of **Q1-3**. No significant variation of the absorption spectra and fluorescence intensity was observed by the subsequent addition of competing anions, which indicated that **Q1-3** has specific selectivity to cyanide anions (Fig. 3).

The absorption and fluorescence titration experiments of sensor **Q1-3** were carried out to explore the interaction between sensor **Q1-3** and cyanide anions. As showed in Figure 4, the variation in the absorption spectrum caused by the gradual addition of cyanide carried out a red shift. Upon the addition of 0–6 equiv of cyanide to the solution

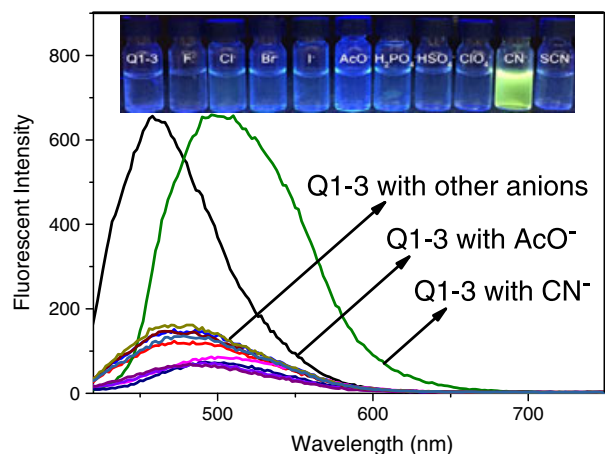


Figure 2. Fluorescent spectra of compound **Q1-3** ($20 \mu\text{M}$) in $\text{DMSO}/\text{H}_2\text{O}$ (1:9, v/v) in the presence of cyanide and other anions (50 equiv.). Inset: photograph showing the change in color of the solution of **Q1-3** in $\text{DMSO}/\text{H}_2\text{O}$ (1:9, v/v, $20 \mu\text{M}$) after addition of cyanide and other anions at room temperature. [Color figure can be viewed at wileyonlinelibrary.com].

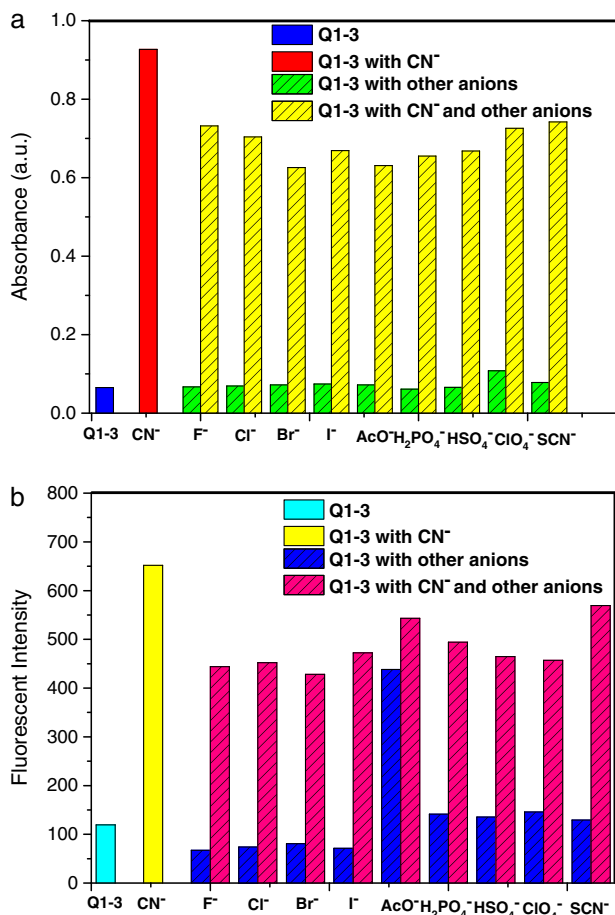


Figure 3. (a) Absorbance data at 400 nm and (b) fluorescence emission data for a 1:50 mixture of **Q1-3** ($20 \mu\text{M}$) and different tetrabutylammonium salts of anions, in $\text{DMSO}/\text{H}_2\text{O}$ (1:9, v/v) solutions at room temperature (excitation wavelength = 400 nm). [Color figure can be viewed at wileyonlinelibrary.com].

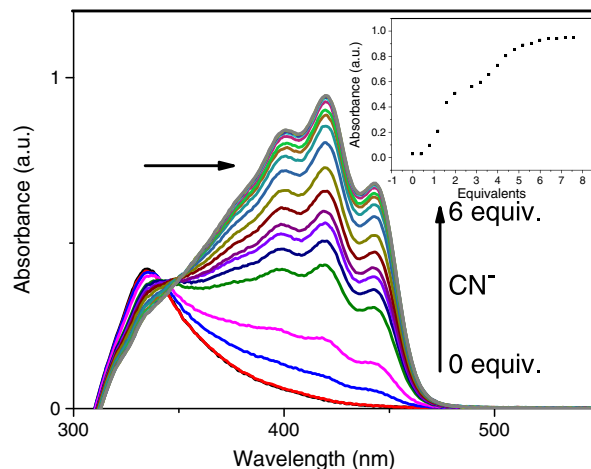


Figure 4. Absorption spectrum of **Q1-3** ($20 \mu\text{M}$) in the presence of different concentration of cyanide in $\text{DMSO}/\text{H}_2\text{O}$ (1:9, v/v) solutions at room temperature. Inset: A plot of absorbance intensity depending on the concentration of cyanide at 418 nm. [Color figure can be viewed at wileyonlinelibrary.com].

of **Q1-3**, the maximum absorption band of **Q1-3** at 335 nm decreased gradually, at the same time, three new absorption bands rapidly appeared at 400, 418, and 442 nm, respectively. The absorption reached maxima after the addition of 6.0 equiv of cyanide anions to the solution of **Q1-3**. The appearance of these three new absorption bands indicated that the intermolecular hydrogen bonds of N–H and O–H were broken by the deprotonation process induced by cyanide anions.

As depicted in Figure 5, the fluorescent peak at 500 nm increased progressively upon the addition of increasing amounts of cyanide anions. More importantly, it was performed with a 78-fold intensity enhancement compared to **Q1-3** when the concentration of cyanide

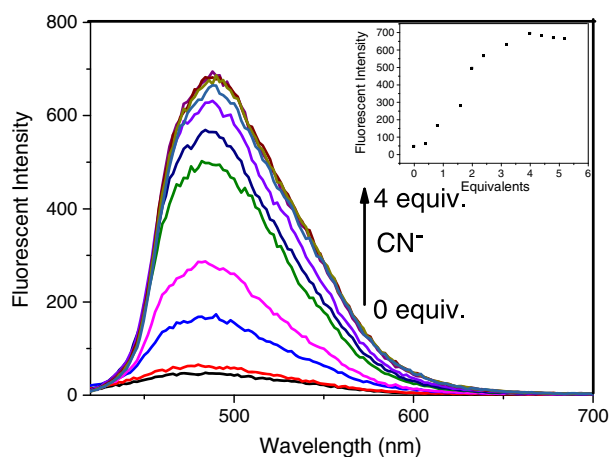


Figure 5. Fluorescent spectrum of **Q1-3** ($20 \mu\text{M}$) in the presence of different concentration of cyanide in $\text{DMSO}/\text{H}_2\text{O}$ (1:9, v/v) solutions at room temperature. Inset: A plot of fluorescent intensity depending on the concentration of cyanide at 500 nm (excitation wavelength = 400 nm). [Color figure can be viewed at wileyonlinelibrary.com].

reached to 4 equiv. Furthermore, the lightless solution of **Q1-3** showed a bright yellow green fluorescent emission in the presence of cyanide anions under an available UV lamp (365 nm). On the basis of these results, it is hypothesized that fluorescent emission change was contributed by the deprotonation of **Q1-3** induced by the cyanide anions. The detection limits of **Q1-3** towards cyanide, obtained according to spectrophotometric titration and fluorescence titration on the basis of $3\sigma/m$, were 3.6893×10^{-10} and 8.0769×10^{-7} M, respectively, as shown in Figures S1 and S2.

Because the pH value affects the charge distribution of receptor **Q1-3** and may change its inherent fluorescence

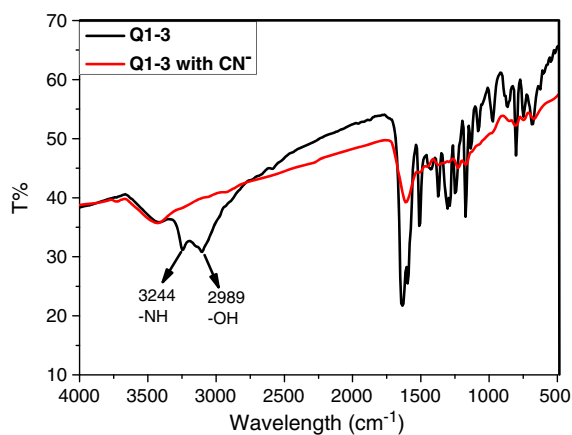


Figure 6. IR spectra of sensor **Q1-3** and after adding cyanide anions in KBr disks. [Color figure can be viewed at wileyonlinelibrary.com].

properties, the effect of various pH on the emission intensity of **Q1-3** in DMSO/H₂O (1:9, v/v) HEPES buffered solution was also studied. As shown in Figure S3, the **Q1-3**-CN⁻ showed significant fluorescence response in the range of pH 4–8. Meanwhile, with the increasing of pH, the receptor's fluorescent gradually increased. These results indicate that **Q1-3** can detect CN⁻ in a range of pH from 4 to 8. Besides, we also detected the response of **Q1-3** towards different anions in DMSO/H₂O (1:9, v/v, pH 7.0) HEPES buffered solution. The result indicated that **Q1-3** can selectively detect CN⁻ in DMSO/H₂O (1:9, v/v, pH 7.0) HEPES buffered solution (Fig. S4).

We further monitored the IR spectra and ¹H-NMR titration to investigate the reaction processes of the probe. IR spectrum of **Q1-3** shows two vibration band at 2989 and 3244 cm⁻¹, which can be assigned to stretching vibrational absorption peaks of -OH and -NH groups in the **Q1-3** molecule, respectively. The vibration band at 1608 cm⁻¹ was attributed to the vibration of -CH=N. However, when **Q1-3** reacted with CN⁻, the stretching vibration absorption peaks of naphthol -OH and -NH group disappeared at 2989 cm⁻¹ and 3244 cm⁻¹, which indicated that **Q1-3** lost the H proton on the acylhydrazone and two phenolic hydroxyl groups after the addition of CN⁻ (Fig. 6).

The results of ¹H-NMR titration experiments also support this presumption. As shown in Figure 7, after adding 0.1 equiv of CN⁻, the singles of phenol -OH on ortho-position and para-position and imide -NH- peak at

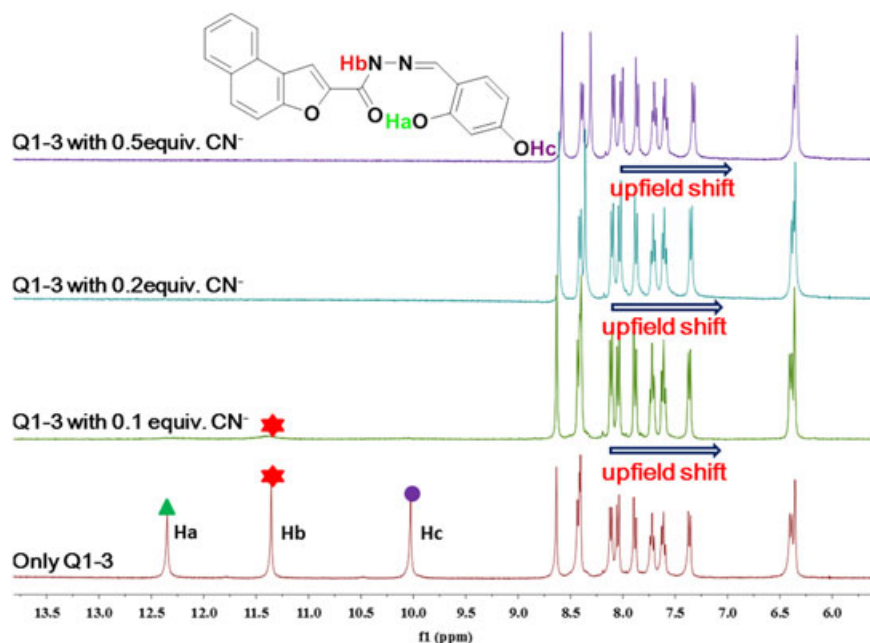


Figure 7. Partial ¹H NMR spectra of **Q1-3** (DMSO-*d*₆) and in the presence of varying amounts of cyanide anions (1 M, D₂O). [Color figure can be viewed at wileyonlinelibrary.com].

12.35, 10.02, and 11.36 ppm decreased and gradually disappeared because of the deprotonation of sensor **Q1-3**. At the same time, the other peaks have an obvious up field shift upon addition of CN^- , indicating that CN^- could take the H protons away *via* deprotonating of the phenol $-\text{OH}$ on ortho-position and para-position and imide $-\text{NH}-$ moiety of **Q1-3**, which enhanced intramolecular electron cloud density and induced the ICT process between the benzene group and naphthofuran group of **Q1-3**.

Therefore, based on the analysis of UV-vis spectra, fluorescence spectra, and IR and $^1\text{H-NMR}$ spectra, we proposed a possible mechanism for the interaction between sensor **Q1-3** and cyanide anions in the optical detection process (Fig. 8). Cyanide could take the H proton away *via* deprotonating in the phenol $-\text{OH}$ on ortho-position and para-position and imide $-\text{NH}-$ moiety of **Q1-3**, which enhanced intramolecular electron cloud density and induced the ICT process between the benzene group and naphthofuran group of **Q1-3**, accompanied with absorption and fluorescence changes.

Furthermore, in order to further investigate the practical utilities of probe in our lives, we used the sensor to detect the CN^- in bitter seeds and sprouting potatoes. Firstly, 100 g of bitter seeds was crushed and pulverized. Then the mixture must be introduced into a flask. Along with this, we added 300 mL water and 0.5 g NaOH, and the obtained mixture should be vigorously stirred for 15 min. After that, the mixture was filtered so as to obtain the cyanide-containing solution (**BSCS**). And we also chose

the sprouting potatoes to implement the following experiment. The sprouting potato (100 g) was first mashed before being soaked in water (200 mL) for 2 days until the extract became turbid. The mixture was filtered, and the filtrate was eluted with 125 mM NaOH solution (100 mL) to obtain the cyanide-containing solution (**SPCS**). As shown in Figure 9(b), upon the addition of **Q1-3** to the two different samples solutions of cyanide anions, the fluorescence intensity of sensor **Q1-3** increased rapidly. The color changes from dim blue to blue-green could be distinguished by the naked eyes under the UV lamp (365 nm) as shown in Figure 9(a). These results showed that we can successfully use the sensor **Q1-3** to detect the cyanide anions in food samples in our daily life.

For convenient use in an on-site visual screening analysis, paper-based sensors and silica gel plates test kits were prepared for visual detection of cyanide. A series of **Q1-3** (0.1 M) DMSO/ H_2O (1:9, v/v) solutions were carefully dropped onto filter paper strips and then dried at room temperature. The test strips containing **Q1-3** were utilized to sense cyanide and other anions. As shown in Figure 10, when cyanide (0.01 M) and the other anions (0.01 M) were added on the test kits, respectively, the obvious color changes were observed only with cyanide solution in visible light and under the 365 nm UV lamp. And potentially competitive anions exerted no influence on the detection of cyanide by the test strips. And potentially competitive anions exerted no influence on the detection of cyanide by the test strips.

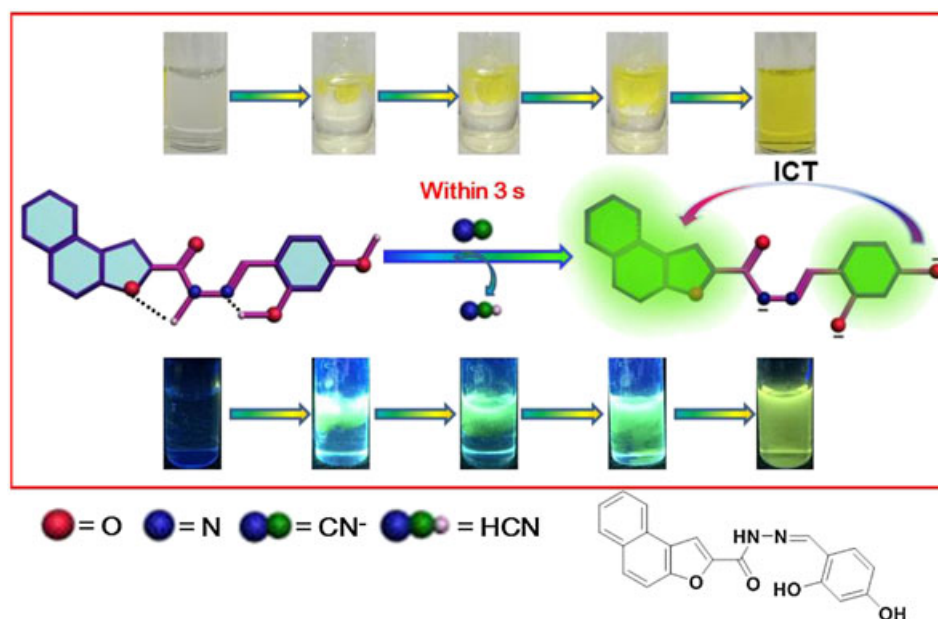


Figure 8. Proposed reaction mechanism of sensor **Q1-3** with NaCN. ICT, intramolecular charge transfer. [Color figure can be viewed at wileyonlinelibrary.com].

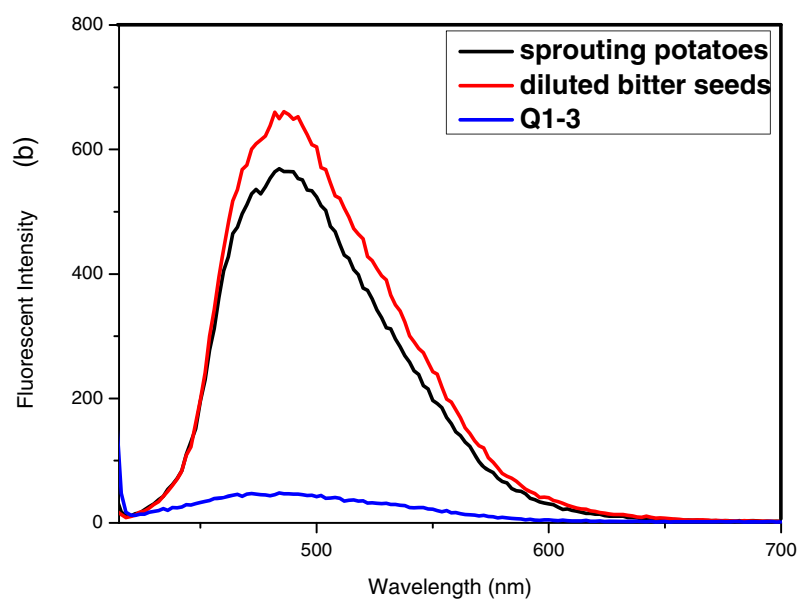
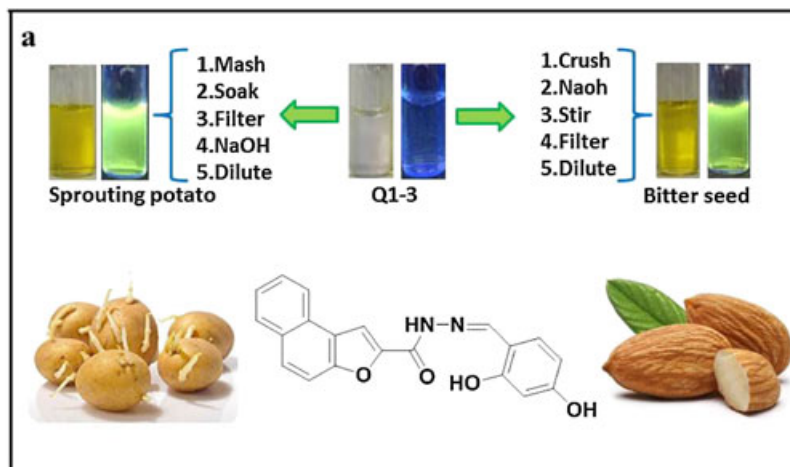


Figure 9. (a) Response photographs of Q1-3 ($20 \mu\text{M}$) in diluted bitter seeds and sprouting potatoes filter. (b) Fluorescence spectral response of Q1-3 ($20 \mu\text{M}$) in diluted bitter seeds and sprouting potatoes filter. [Color figure can be viewed at wileyonlinelibrary.com].

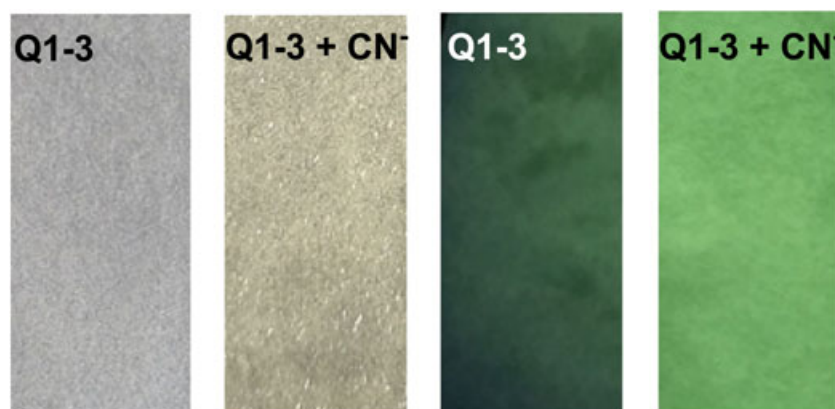


Figure 10. Photographs of Q1-3 and the response of cyanide on test papers in visible light and under irradiation at 365 nm. [Color figure can be viewed at wileyonlinelibrary.com].

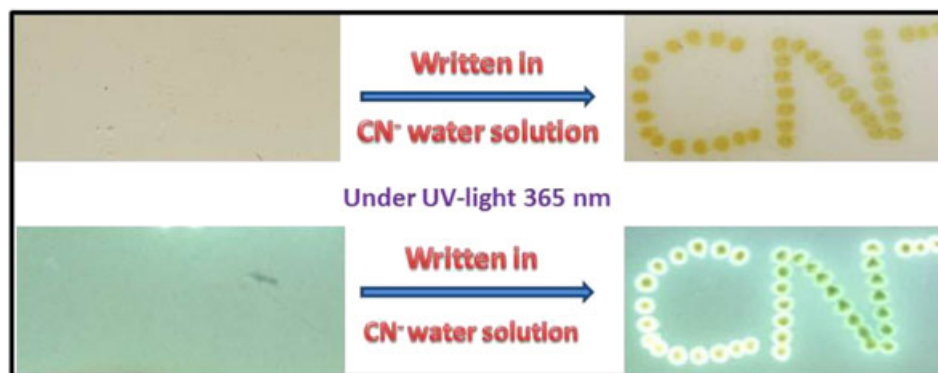


Figure 11. Photos of the silica gel plates utilized to sense cyanide in aqueous solution in visible light and under irradiation at 365 nm by a UV lamp. [Color figure can be viewed at wileyonlinelibrary.com].

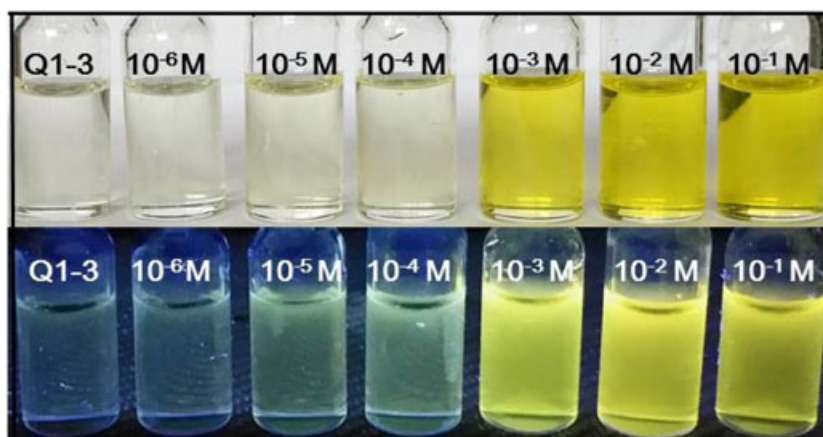


Figure 12. Above: photographs of **Q1-3** in DMSO/H₂O (1:9, v/v) solutions after immersion with different concentration of cyanide and only **Q1-3** in visible light. Below: photographs of **Q1-3** in in DMSO/H₂O (1:9, v/v) solutions after immersion with different concentration of cyanide and only **Q1-3** under irradiation at 365 nm. [Color figure can be viewed at wileyonlinelibrary.com].

In addition, we also prepared silica gel plates test kits by silica gel plates into DMSO/H₂O (1:9, v/v) solutions of **Q1-3** (0.1 M) and then drying in air. For instance, as shown in Fig. 11 when we dipped on the silica gel plate, which contains **Q1-3** by a brush containing the aqueous solution of cyanide, a pale yellow mark can be observed in visible light, and a yellow green fluorescent image appeared under the 365-nm UV lamp.

Furthermore, in order to conform the naked-eye detection ability of **Q1-3** in aqueous solution, we also examined the naked-eye detection limits of **Q1-3**. As shown in Figure 12, we prepared a series of solutions, which containing different concentrations of cyanide. The naked-eye detection limits of **Q1-3** are 1×10^{-5} M in visible light and 1×10^{-5} M under the UV lamp (365 nm). Therefore, the probe could conveniently detect cyanide in solutions by naked eyes at very low concentrations.

CONCLUSION

In conclusion, we designed and synthesized an ICT-based sensor **Q1-3** for rapid response and superb selective detection of cyanide anions in aqueous solutions DMSO/H₂O (1:9, v/v). The sensor demonstrated advantages for cyanide anion detection such as dual-channel and turn-on fluorescent emission, low detection limits both in UV-vis absorption spectrum and fluorescent emission spectrum in DMSO/H₂O (1:9, v/v) solutions, and the successful application in test kits, silica gel plates, and food samples. It is also noteworthy that the choice of the sensor **Q1-3** allows rapid detection of cyanide in terms of real time, as the time response (within 3 s) here is faster compared to that of the reported systems. This sensor allows a simple and effective way for on-site visual detection of cyanide anions in natural environment.

Acknowledgments. This work was supported by the National Natural Science Foundation of China (Nos. 21661028, 21662031, and 21574104), the Program for Changjiang Scholars and Innovative Research Team in University of Ministry of Education of China (IRT 15R56).

REFERENCES AND NOTES

- [1] Tarafdar, D.; Saha, I.; Ghosh, K. *Tetrahedron Lett* 2017, 58, 2038.
- [2] Dvivedi, A.; Kumar, S.; Ravikanth, M. *Sens Actuators B* 2016, 224, 364.
- [3] Kaushik, R.; Ghosh, A.; Singh, A.; Gupta, P.; Mittal, A.; Jose, D. A. *ACS Sens* 2016, 1, 1265.
- [4] Wang, L.; Li, L.; Cao, D. *Sens Actuators B* 2017, 241, 1224.
- [5] Dong, M.; Peng, Y.; Dong, Y. M.; Tang, N.; Wang, Y. *W. Org Lett* 2012, 14, 130.
- [6] Sun, Y.; Hu, J. H.; Qi, J.; Li, J. B. *Spectrochim Acta Part A Molecular and Biomolecular Spectroscopy* 2016, 167, 101.
- [7] Huo, F.; Kanga, J.; Yin, C.; Chao, J.; Zhang, Y. *Sens Actuators B* 2015, 215, 93.
- [8] Wang, P.; Yao, Y.; Xue, M. *Chem Commun* 2014, 50, 5064.
- [9] Wang, L.; Zheng, J.; Yang, S.; Wu, C.; Liu, C.; Xiao, Y.; Li, Y.; Qing, Z.; Yang, R. *ACS Appl Mater Interfaces* 2015, 7, 19509.
- [10] Badugu, R.; Lakowicz, J. R.; Geddes, C. D. *J Am Chem Soc* 2005, 127, 3635.
- [11] Zelder, F.; Tivana, L. *Org Biomol Chem* 2015, 13, 14.
- [12] Kaur, K.; Saini, R.; Kumar, A.; Luxami, V.; Kaur, N.; Singh, P.; Kumar, S. *Coord Chem Rev* 2012, 256, 1992.
- [13] Pramanik, S.; Bhalla, V.; Kumar, M. *ACS Appl Mater Interfaces* 2014, 6, 5930.
- [14] Fielden, P.; Smith, S. J.; Alder, J. F. *Analyst* 1986, 111, 695.
- [15] Rubio, R.; Sanz, J.; Rauret, G. *Analyst* 1987, 112, 1705.
- [16] Safavia, A.; Malekia, N.; Shahbaazia, H. R. *Anal Chim Acta* 2004, 503, 213.
- [17] Shiraiishi, Y.; Nakamura, M.; Hayashi, N.; Hirai, T. *Anal Chem* 2016, 88, 6805.
- [18] Jang, H. J.; Jo, T. G.; Kim, C. *RSC Adv* 2017, 7, 17650.
- [19] Shiraiishi, Y.; Hayashi, N.; Nakahata, M.; Sakai, S.; Hirai, T.; Jo, J. *RSC Adv* 2017, 7, 32304.
- [20] Liu, Y. W.; Kao, M. X.; Wu, A. T. *Sens Actuators B* 2015, 208, 429.
- [21] Maurya, N.; Singh, A. K. *Sens Actuators B* 2017, 245, 74.
- [22] Hu, J. H.; Li, J. B.; Qi, J.; Sun, Y. *New J Chem* 2015, 39, 4041.
- [23] Jain, A.; Gupta, R.; Agarwal, M. *J Heterocyclic Chem* 2017, 54, 2808.
- [24] Yu, G.; Zhang, Z.; Han, C.; Xue, M.; Zhou, Q.; Huang, F. *Chem Commun* 2012, 48, 2958.
- [25] Huo, F.; Zhang, Y.; Ning, P.; Meng, X.; Yin, C. *J Mater Chem B* 2017, 5, 2798.
- [26] Yang, L.; Li, X.; Yang, J.; Qu, Y.; Hua, J. *ACS Appl Mater Interfaces* 2013, 5, 1317.
- [27] Kang, J.; Song, E. J.; Kim, H.; Kim, Y. H.; Kim, Y.; Kim, S. J.; Kim, C. *Tetrahedron Lett* 2013, 54, 1015.
- [28] Wang, L.; Zhu, L.; Li, L.; Cao, D. *RSC Adv* 2016, 6, 55182.
- [29] Shi, B.; Jie, K.; Zhou, Y.; Zhou, J.; Xia, D.; Huang, F. *J Am Chem Soc* 2016, 138, 80.
- [30] Lin, S.; Liu, S.; Ye, F.; Xu, L.; Zeng, W.; Wang, L.; Li, L.; Beuerman, R.; Cao, D. *Sens Actuators B* 2013, 182, 176.
- [31] Guo, Y.; Huo, F.; Yin, C.; Kang, J.; Li, J. *RSC Adv* 2015, 5, 10845.
- [32] Shi, B.; Jie, K.; Zhou, Y.; Xia, D.; Yao, Y. *Chem Commun* 2015, 51, 4503.
- [33] Ji, X.; Yao, Y.; Li, J.; Yan, X.; Huang, F. *J Am Chem Soc* 2013, 135, 74.
- [34] Luo, X.; He, X. D.; Zhao, Y. C.; Chen, C.; Chen, B.; Wu, Z. B.; Wang, P. Y. *J Heterocyclic Chem* 2017, 54, 2650.

SUPPORTING INFORMATION

Additional Supporting Information may be found online in the supporting information tab for this article.